Explicit Derivation of Dark Thermionic Current Densities in III-V Multiquantum Well Infrared Photodetectors

ARGYRIOS C. VARONIDES
Physics and Electrical Engineering Department
University of Scranton
800 Linden Street, Scranton, PA 18510
United States

Abstract: We propose an analytic calculation of the dark current density for GaAs/A1GaAs thick barrier quantum well infrared photo-detectors (QWIP's). We evaluate the dark current component, by integrating (a) drift velocity of the carriers via their kinetic energy (b) the non-tunneling probability factor 1-T (E) (c) the Fermi factor and (d) the 3-d density of states (DOS) of the multiple quantum well structure. We find that the dark currents depend on the temperature T, applied bias $V_{b,}$ aluminum molar ratio (and hence barrier height Δ), cut-off energy $\Delta E=E_c-E_F$ and peak wavelength according Incorporation of superlattices in infrared photodetectors leads to a $T^{3/2}$ term, which is due to the 2-dimensional electronic gas (2DEG) of the wells. We find that dark thermionic current densities (a) increase dramatically with temperature under fixed bias levels (42 mA/cm^2 at 80°K & 30 mV and 1.512 A/cm^2 at 100°K & 30mV) (b) increase with applied voltage at fixed temperatures (e.g. 0.0018 A/cm^2 to 0.7445 A/cm^2 at 80°K, from 10mV to 50mV), both at peak wavelengths of 10μm.

Keywords: Quantum wells, infrared photo-detectors, thermionic emission

1 Introduction

Quantum well structures have become vital parts of a new class of detectors in the infrared [1] Epitaxial techniques for III-V multi-layered devices have reached high levels of maturity, and thus multi-junction quantum well photo-detectors can be fabricated routinely. Multi-quantum well photo-detectors with thin quantum wells and thick barriers ensure thermal escape of carriers from the wells in the continuum, thus producing non-zero thermal currents. In this communication we provide a set of analytical calculations of the dark currents and we report on their explicit dependence on temperature T. In doing this, we emphasize the importance of the two-dimensional electronic gas (2DEG) of trapped carriers in the wells, assuming moderate doping levels. The detector is in essence a type-I superlattice [GaAs-A1GaAs], embedded between two layers of wide gap material (36%-A1GaAs).

2 Structure and Formulation

The design discussed here includes the following features: (a) a superlattice structure with GaAs as the narrow gap material and A1GaAs (x-36%) as the wide band-gap material respectively (b) the well widths are taken to be 30 Angstroms, which ensures formation of single energy levels in the wells, while the second excited level is at the edge of the barrier in a quasi-bound status. Thermally escaping carriers from the wells will contribute to the dark thermal currents, while tunneling will depend upon the thickness of the barriers. The main goal here is to provide a general result for the dark thermal currents in QWIP's, where the barrier widths L_0 are chosen to be above 400A and the A1 molar ratio is assumed to be 36%, providing potential steps (barrier) of 0.3eV. The multi-quantum well thermal current density is evaluated from the general J=nqv regime where n is the carrier concentration per unit volume, v is the drift velocity of the carriers. This regime is generalized below, based on three conditions that ought to be satisfied. These are:

(i) all the carriers trapped in the superlattice minibands need to be accounted for, via the density of energy states available in the quantum well
(ii) the probability of occupation of these states needs to be explicitly known, and
(iii) the probability for thermal escape.

$$J_{\mathrm{TH}} = q\int_{E_0}^{E_1} dEg(E)(f(E-E_{F1}) - f(E-E_{Fr}))v(E)(1-T(E)) \qquad (1)$$

Where q is the electronic charge, g(E) is the three-dimensional density of states (3-D DOS) of the quantum well structure, [f(E-E_{F1})-f(E-E_{Fr})] is the Fermi-Dirac distribution, expressed as a function of the quasi-Fermi levels, and through the applied voltage V_b in the Maxwell-Boltzmann approximation (see expression (4) below(1-T(E) is the escape probability T(E) factor is negligible, while the complete format given by (1) can be used in the different case of thin wells and thin barriers). The integration in (1) is taken from the ground state to the first excited state thus covering the energy distance from the localized miniband electrons to continuum. v(E) is the drift velocity of the escaping carriers, and it is expressed in terms of the carrier kinetic energy. The integration is performed over the energy distance between the ground state E_0 and the first excited state E_1, which (due to the adopted device geometry) is forced to be aligned with the conduction edge of the wide gap semiconductor, thus leading to *bound to quasi-continuum* transitions. The transition energy is E_1-E_0 (eV), and thus the peak wavelength λ_p is given by the following:

$$\lambda_p(\mu m) = \frac{1.24}{E_1(eV) - E_0(eV)} \qquad (2)$$

The various parameters mentioned above are:

$$g(E) = \frac{m^{\cdot}}{\pi h^2 L_w} \qquad v(E) = \sqrt{\frac{2}{m}}\sqrt{E - E_0} \tag{3}$$

$$f(E - E_{F1}) - f(E - E_{Fr}) = exp(-(E - E_{Fr})/kT)\left(exp(\frac{qV_b}{kT}) - 1\right) \tag{4}$$

L_b is the barrier thickness and k_b (m^{-1}) is:

$$k_b = \sqrt{\frac{2m^*(\Delta - E_0)}{\hbar^2}} \tag{5}$$

Expression (1) after the insertion of (2), (3), and (4) and direct integration leads to:

$$J_{TH} = \frac{2q\sqrt{2m^*}}{\pi\hbar^2 L_W}(kT)^{3/2}(e^{qVb/kT} - 1)e^{-(E_0 - E_{Fr})}/kT \tag{6}$$

From (6) we see that, given the pre-selected geometry of the superlattice [i.e. widths (L_w, L_b) and barrier heights, due to molar ratios], the dark current density depends on temperature as $\mathbf{T^{3/2}}$, while the cut-off energy is implicitly included in the second exponential factor, since the second exponent in (6) can be re-written as (see Fig. 1):

$$E_0 - E_{Fr} = (E_o - E_{C1}) + (E_{C1} - E_{Fr}) \tag{7}$$

Where the first term in (7) is the first mini-band relative to the bottom of the quantum well and the second term is the cut-off energy [3] or simply the distance of the Fermi level from the conduction band of the narrow gap material. Expression (7) is further explored in terms of the peak wavelength as follows:

$$E_0 - E_F = \Delta - \left(\frac{1.24}{\lambda_p}\right) + (E_{cl} - E_F) \tag{8}$$

This is because

$$E_0 - E_{c1} = \Delta - (E_1 - E_0) = \Delta - \frac{1.24}{\lambda_p(\mu m)} \tag{9}$$

And where (Fig. 1) the miniband E_1 (quasi-bound) coincides with the conduction band-edge E_{c2}. Under (7) and (8), (6) becomes:

$$J_{TH} = J_{0^e}{}^{-(\Delta - \frac{1.24}{\lambda p})/kT} T^{3/2}\left(e(qV_b/kT)-1\right)e\left(-(\frac{E_{c1}-E_F}{kT})\right) \qquad (10)$$

Where

$$J_0 = \left(\frac{(2k)^{3/2} q\sqrt{m^*}}{\pi\hbar^2 L_w}\right)$$

Immediate conclusions from (10) are that dark thermionic currents depend on temperature T, not only via the exponential factors [2,3,4] but, in addition, through a $T^{3/2}$ term as well. The latter $T^{3/2}$ dependence is due to the second order dimensionality (2-d DOS) of the density of states pattern of the quantum wells.

3 Results

In the following, some representative results are shown at two temperatures: 80ºK, and 120ºK respectively, and under low bias V_b. Table 1 depicts variation of dark currents under fixed temperature but at varying biases, and Table 2 depicts values of dark currents at varying temperatures under a fixed bias:

Table 1. Dark currents of the A1GaAs/GaAs superlattice photodetector vs V_b

V_0 (mV)	J_d (A/cm^2) @80ºK	J_d (A/cm^2) @120ºK
10	0.0018	3.34
20	0.0096	12.09
30	0.0422	34.97
40	0.1782	94.83
50	0.7445	251.39

[A] ratio: 36% / 30A/10μm/80K & 120K]

Note that the dark currents increase sharply as the applied voltage increases from 10mV to 50mV. Note also that for reverse biases of the same range as the ones shown in Table 1, the dark currents remain at 5.89 x 10^{-4} A/cm^2 at 80K, while similar behavior is found for the second temperature (120K) but at 2.07 A/cm^2. This is because the exponential term that includes the bias (see (10) becomes much less than unity, thus freezing the values of the dark currents. Dark current variation with temperature under two fixed biases (+30mV and +50mV) is shown in Table 2. For instance, at 100°K there is a factor of ten increase in the current density as the applied voltage increases from 30mV to 50mV.

Table 2. Dark currents of the A1GaAs/GaAs superlattice photodetector vs T.

T (°K)	J_d (A/cm^2)@30mV	J_d (A/cm^2) @50mV
80	0.042	0.74
90	0.570	7.10
100	1.512	15.60
120	34.97	251.39
130	106.40	667.96

[A1 ratio: 36% / 30A/10μm/30mV&50mV]

It is seen that as the temperature increases from 80K to 130K, the dark current increases dramatically, under forward bias, while the reverse current densities are at almost fixed values just as in the cases mentioned above. The position of the Fermi level E_{Fr} (Fig. 1) varies relative to the bottom of the quantum wells, as a function of temperature T. It turns out, that the difference E_{Fr}-E_{c1} is + 19.6meV and +22.86meV within the quantum wells and for 80°K and 120°K respectively, and for well doping levels at ~10^{18} cm^{-3}. The corresponding cut-off wavelengths λ_c, relative to the quasi-bound eigen-energy E_1 are 4.42 μm and 4.47 μm respectively, while peak wavelengths are at 10μm. As it is expected from (10), there is no net current under zero bias.
Fig. 1, shown below, depicts the main parameters involved in the design, under zero bias. One can see the wide-gap and narrow-gap layers forming the quantum wells (30A well width at 36% A1 ratio). Transitions to quasi-bound states are denoted by peak wavelength λ_p through conduction band discontinuity Δ.

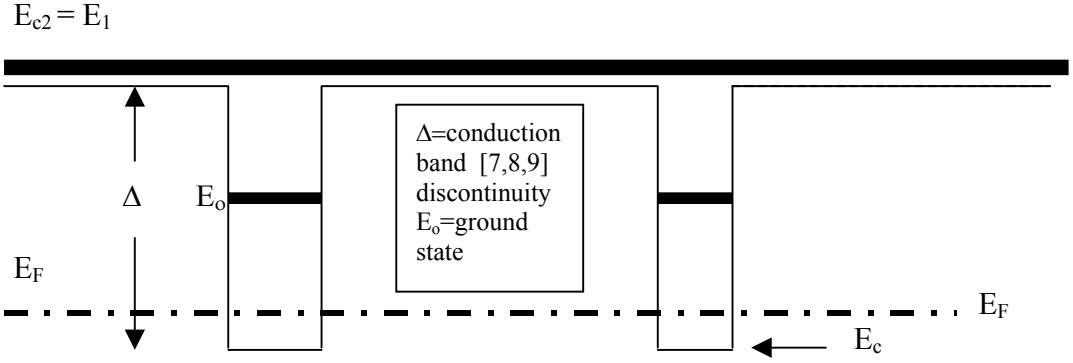

Fig. 1 Main parameters of the superlattice-based QWIP, with $E_0 \rightarrow E_{Continum}$ transitions.

Note the finite (non-zero) width of both the ground and first excited states: selected geometry engineering as such shown above, may lead to a coincidence of upper conduction band and excited states, so that first order transitions are very possible under illumination. Quantum wells are grown far from each other (more than 500A) so that tunneling is minimized. Fermi levels are forced "inside" the quantum wells, thus ensuring carrier excitations at a wider wavelength ranges. Also, design as in the Fig. 1 above, ensures only one energy state inside the quantum well, and the second at the edge of the

conduction band of the wider band-gap material, so that in essence thermally escaping electrons may "roll" down the slope in an easier fashion. The latter reduces scattering and carrier trapping, thus leading to improved transport properties (work on such benefits is under way).

4 Summary

We have presented the dependence on temperature T on dark current, which is produced by escaping carriers from the single-eigen-energy doped quantum wells to the quasi-bound eigen-energy at the edge of the barriers (of height Δ). The main result of the derivation is that dark currents *do depend on the temperatures via a* $T^{3/2}$ *exp* $(-\Delta E/kT)$ factor, where the exponent includes the design parameters of the superlattice structure. These parameters are (i) the barrier height (ii) the splitting of the quasi-Fermi levels via the applied voltage (iii) the peak wavelength (iv) the cut-off energy (iv) scattering and quantum well trapping is expected to be minimized when electron transport is performed through the second energy level which shares the conduction band continuum and the upper edge of the wide-gap conduction band.

References:

[1] B.F. Levine, *III-V Quantum Wells and Superlattices* (P. Bhattacharya editor), IEE No 15, 1996.
[2] B.F. Levine, A. Zussman et al, J. Appl. Phys 72 (1992) 4429.
[3] K.M. Bandara, B.F. Levine, and M.T. Asom. J. Appl. Phys. 74 (1) (1993) 346.
[4] B.F. Levine, et al, J. Appl. Phys. 56 (9) (1990) 851.
[5] K.K. Choi et al, Appl. Phys. Lett. 65 (13) (1994) 1703.
[6] K.K. Choi, The Physics of quantum Well Infrared Photodetectors, (World Scientific, 1997).
[7] J. Tersoff, *Heterojunction Band Discontinuities,* F. Capasso, and G. Margaritondo eds, North Holland Physics Publishers, 1987, pp. 3-57.
[8] M. Altarelli, *Heterojunctions and Semiconductor Superlattices,* G. Allan, G. Bastard, N. Bocara, M. Lannoo and M. Voos Eds, Springer-Verlag, 1986.
[9] G. Bastard, J.A. Brum, *IEEE, JQE-22,* 1986, pp. 1853-1869.
[10]